Received: 19 May 2022 | Revised: 4 September 2022 | Accepted: 11 September 2022

DOI: 10.1002/dep2.208

The Depositional Record Open Access
A journal of the International Association of Sedimentologists
WILEY

ORIGINAL ARTICLE

Spatial variations in sediment production and surface transformations in subtropical fluvial basins (Caculuvar River, south-west Angola): Implications for the composition of sedimentary deposits

Armanda Trindade Cruz[1] | **Pedro Alexandre Dinis**[1] | **Mavro Lucic**[2] | **Alberto Gomes**[3]

[1]Department of Earth Sciences, University of Coimbra, MARE-Marine and Environmental Sciences Centre/ARNET—Aquatic Research Network, Coimbra, Portugal

[2]Department for Marine and Environmental Research, Ruđer Bošković Institute, Zagreb, Croatia

[3]Department of Geography, CEGOT—Centre of Studies in Geography and Spatial Planning, University of Porto, Porto, Portugal

Correspondence
Pedro Alexandre Dinis, Department of Earth Sciences, University of Coimbra, 3030 790 Coimbra, Portugal.
Email: pdinis@dct.uc.pt

Funding information
Fundação para a Ciência e a Tecnologia

Abstract

Several compositional features of sedimentary deposits can be used to reconstruct environmental conditions of source areas. In this research, bulk X-ray diffraction mineralogy, heavy and clay mineral assemblages and geochemistry obtained for modern deposits of the Cunene River and its tributaries Caculuvar–Mucope are integrated with geological/geomorphological characteristics of respective catchment areas to evaluate to what extent sediment production is spatially variable and source materials are differently affected by exogenous transformations. Detrital sources can be classified into four main types based on sediment composition: felsic, mafic, recycled and mixed. Source contributions obtained with unmixing models using distinct input data reveal some disagreements, with heavy mineral assemblages pointing to higher mafic contribution and bulk XRD-mineralogy favouring the recycled sedimentary component. However, the three datasets coincide showing a lower supply from the Kalahari Basin than the large outcropping areas of its sedimentary units would suggest, which is attributed to the relatively low rainfall and relief in this region. Where multiple depositional cycles are involved in sediment production the composition of the river deposits, even their clay fractions, will not reflect coeval weathering transformations and an underestimation of the mafic component probably occurs. This research reveals how exogenous processes may deviate the composition of the produced sediment from a simple weighted by outcropping area average of the source units and compromise (palaeo)environmental interpretations based on sediment composition.

KEYWORDS

geochemistry, mineralogy, provenance, recycling effects, source contributions

1 | INTRODUCTION

The composition of fluvial deposits is determined by source area geology coupled with weathering and erosional processes during the sediment cycle, which depends in turn on regional orography and climate (Arribas et al., 2007; Dixon et al., 2012; Johnsson & Basu, 1993; Morton & Hallsworth, 1999; Rasmussen et al., 2011). Differences in these environmental features account for heterogeneous sediment production within catchment areas. Because the mineral constituents of source units are not equally vulnerable to chemical decomposition and mechanical disintegration and are not transported the same way, the composition of daughter sediment cannot faithfully reflect the composition of the units cropping out in the catchment areas. In other words, chemically and mechanically stable minerals, such as quartz, will become enriched through sediment cycles (Garzanti et al., 2020; Suttner et al., 1981). Consequently, other minerals tend to become under-represented in sedimentary deposits relative to primary source units.

Complexity increases where multiple source rocks are present. It has been demonstrated that the production of sediments of different grain sizes strongly depends on primary source units. For example, granitoids can generate large amounts of sand-sized material, while basalts are major mud suppliers but cannot create much sand (Garçon & Chauvel, 2014; Garzanti et al., 2021; Maharana et al., 2018). However, different contributions of mafic and felsic plutonic rocks that lack the extremely vulnerable glassy component of volcanic rocks were not investigated in detail. It is also known that the transformations responsible for shifting the composition of end products from primary source materials tend to be most intense where warm and wet conditions promote chemical decomposition (Garzanti et al., 2013a; Johnsson et al., 1991; Savage & Potter, 1991). In particular if regional relief is smooth and a longer time for weathering reactions is available (Gabet & Mudd, 2009; Riebe et al., 2004; West et al., 2005). Regardless of present-day geomorphological conditions, a renewed removal of the less mechanically and chemically stable elements occurs if sediment material has passed through a succession of depositional cycles (Cox et al., 1995; Dinis et al., 2020; Gaillardet et al., 1999; Garzanti et al., 2020).

The present investigation focusses on the Cunene River and, in particular, its tributary Caculuvar in subtropical south-west Angola, which comprises two trunk rivers: the Caculuvar and the Mucope. The drainage basin of Mucope is entirely located in the Kalahari Basin with an infill dominated by Cenozoic deposits, while the Caculuvar drains in similar proportions felsic (13%) and mafic (14%) plutonic rocks, and wide areas with sedimentary and metasedimentary units. A set of compositional data, including geochemistry, bulk mineralogy, clay mineralogy and heavy mineral assemblages, obtained for present-day deposits of the Caculuvar–Mucope and Cunene rivers are analysed in combination with the geology and geomorphology of their catchment areas. The studied area, spreading through sectors with contrasting geology/geomorphology is excellent for investigating the processes controlling variable sediment production. Particular emphasis is given to the relative contributions of different source units and how exogenous processes may deviate the composition of daughter deposits from source composition.

2 | REGIONAL SETTING

The Cunene River drains the Angola Block of the Congo Craton (De Waele et al., 2008; Hanson, 2003), cropping out to the west, and the covering sequences from the Kalahari Basin, mostly to the east and south (Haddon & McCarthy, 2005). The Caculuvar River is the biggest tributary of the Cunene River (Figure 1), with a 273 km long drainage basin that extends for 25,322 km^2. Two main geological units drained by the Cunene River upstream of the Caculuvar confluence can be considered for the Angola Block. (1) A Palaeoproterozoic (*ca* 2.2–2.0 Ga; Carvalho et al., 2000; Pereira et al., 2011) peraluminous leucocratic granite locally called 'regional granite' (Carvalho, 1984) crops out mainly in northern locations. These basement units are overlain in the north-west tip of the Caculuvar drainage basin by the Chela Group, composed of a siliciclastic succession with intercalated volcanoclastic rocks, and the Leba Formation, with dark dolomitic limestones (Correia, 1976). (2) In an elongated fringe bordering the Kalahari Basin to the west and north-west, crop out the Mesoproterozoic mafic igneous rocks of the Cunene Complex of south-west Angola, also known as the gabbro-anorthosite complex (Carvalho et al., 2000; Ernst et al., 2013; Mayer et al., 2004; Morais et al., 1998). This unit, coupled with its counterpart in Namibia, is Africa's largest mafic complex. In places, A-type red granites usually trending SW–NE were emplaced with the mafic complex (Drüppel et al., 2007).

The sedimentary infill of the Kalahari Basin can be broadly subdivided into the Kalahari Group with aeolian and fluvial deposits dated to late Cretaceous to Cenozoic age (Araújo et al., 1992; Haddon & McCarthy, 2005) and a series of Quaternary loose sands with variable amounts of fine-grained particles, which result from aeolian and fluvial remobilisation of the Kalahari Group. A prominent geomorphological feature of this region is the lower Cunene planation surface that slightly dips south-east.

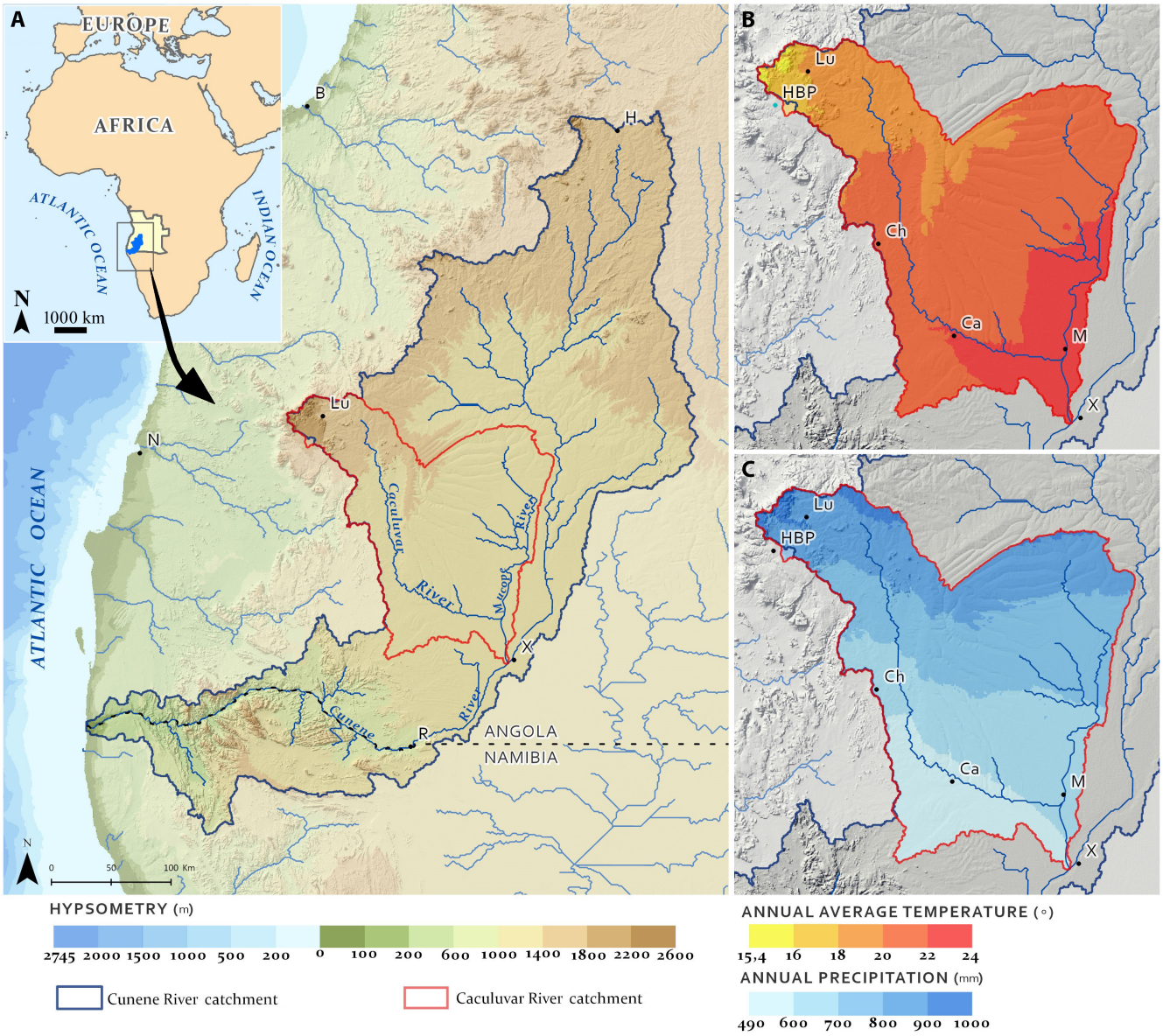

FIGURE 1 Location of the studied area in south-west Africa. (A) The Caculuvar–Mucope river system and the Cunene drainage basin. General patterns of rainfall (B) and temperature (C) in the Caculuvar-Mucope drainage area. HBP: Humpata–Bimbe plateau; Lu: Lubango; Ch: Chibia; C: Cahama; M: Mucope; X: Xangongo.

Two trunk rivers can be considered in the Caculuvar drainage basin: the Mucope, to the east, and the main trunk of the Caculuvar, to the west, with the confluence between the two taking place only *ca* 10 km upstream of the Cunene River (Figure 2). The drainage basin of the Caculuvar is elongated, crossing different units of the Angola Block. The lithic contrast in this region of the Angola Block is responsible for several residual reliefs interspersed with extensive flat areas (Feio, 1981). The Mucope River drains exclusively sedimentary units of the Kalahari Basin. It has a broadly circular catchment area and longer tributaries in its western flank.

Strong climate seasonality is observed in south-west Angola, with a warmer wet season from October to April and a colder dry season from May to September (Huntley, 2019). At these latitudes, the Angola Low is responsible for summer rains (Cook et al., 2004; Crétat et al., 2019), while the El Niño Southern Oscillation primarily accounts for significant rainfall variations at interannual scales (Dieppois et al., 2015). Despite registering a tropical thermal regime mediated by the catchment's mountains (monthly average close to 22°C), the average temperature increases east and south. Annual rainfall varies in the opposite direction. On average, the southern sectors of the Caculuvar and Mucope catchments receive about 450–500 mm of precipitation per year while to the north, particularly in the mountainous sector of the Caculuvar River basin, *ca* 1000 mm is usually recorded (Figure 2). According to the Köppen–Geiger

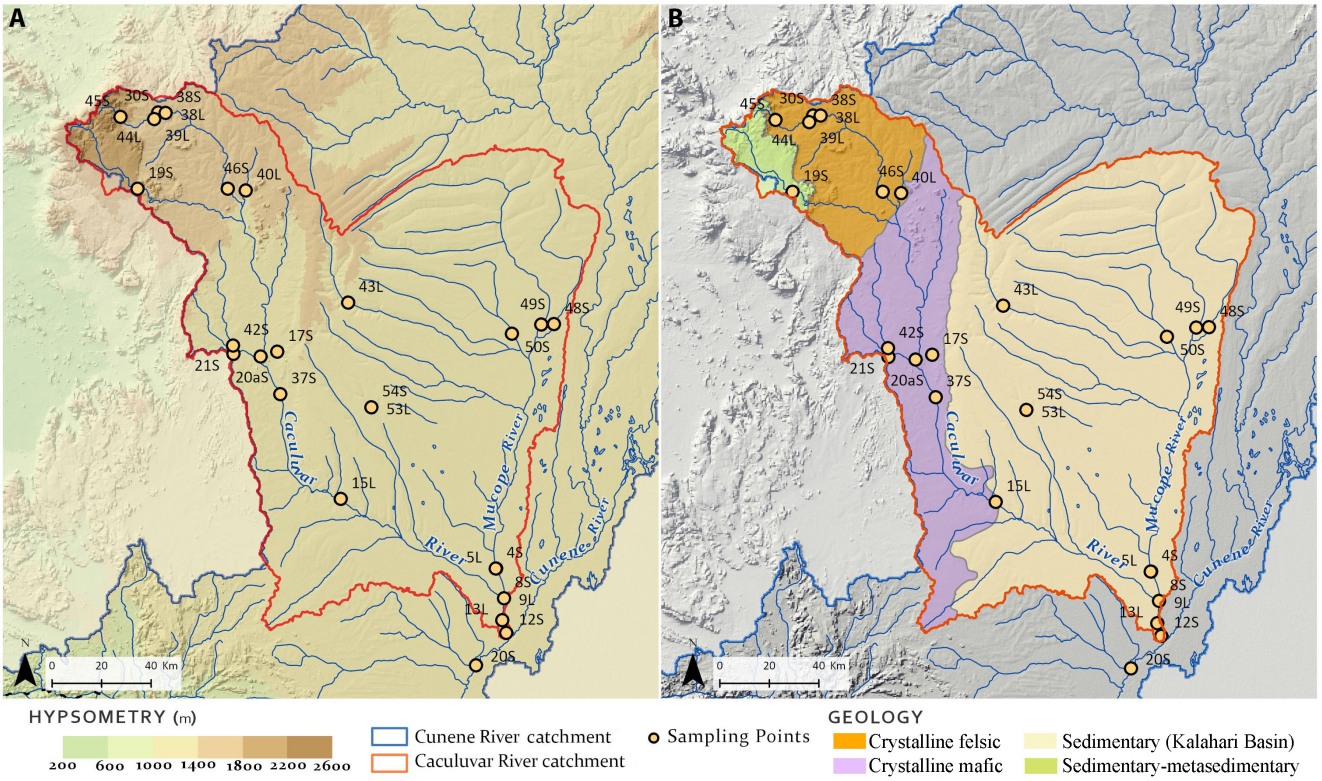

FIGURE 2 Orography (A) and geology (B) of the Caculuvar–Mucope catchment area and location of sampling sites. Geology is based on the geological map of Angola, scale 1/1,000,000 (Araújo et al., 1992). L and S refer to mud and sand samples.

classification (http://koeppen-geiger.vu-wien.ac.at/present.htm), climate is sub-tropical highland (Cwb) in the north-west mountainous sector, passing southwards to hot semi-arid (Bsh).

3 | METHODS

3.1 | Geomorphological analysis

The geological data used in this research came from the Geological Map of Angola, at a scale of 1/1,000,000, sheet 3 (Araújo et al., 1992). The delimitation of the basins, sub-basins, hydrographic network and geomorphological analyses were done applying the geospatial tools of QGIS and SAGA software. All the topographic, hydrographic and morphometric parameters were based on the SRTM altimetric data (30 m of pixel size) provided by the US Geological Survey (USGS; https://earthexplorer.usgs.gov/). The hydrographic network was generated considering the D8 flowing accumulation model and classified according to the Strahler hierarchy (level 7). To characterise and differentiate the source regions, several geomorphic parameters were considered. Relative relief, expressing the difference in height between the highest and the lowest points in a determined surface grid area, was obtained by the process described in Florinsky (2016). The valley depth was calculated in SAGA GIS (https://saga-gis.sourceforge.io/saga_tool_doc/), and considered the difference between the elevation and an interpolated ridge level. Morphometric parameters were calculated for each catchment area and the main types of source units (felsic igneous, mafic igneous, sedimentary and meta-sedimentary).

The selection of the sampling sites was carried out according to geomorphological and geological criteria, making sure that rivers draining almost exclusively single lithological units and main rivers with distinct upstream geology were included. Considering these criteria, field locations were first defined by observing imagery from the Google Earth and Terra Incognita platforms and then transferred to a geodatabase for use in the field. Following this geological and geomorphological assessment, river sediments were collected in selected stretches of the Caculuvar and Mucope drainage basins.

3.2 | Sediment sampling and composition

Wherever possible, samples of sand and mud deposits were collected in fluvial channels and river banks (Figure 2). Previous to compositional analysis, mud and sand dominated deposits were sieved to remove the fractions >0.035 and >2 mm, respectively. In addition, all

sediments that hold significant amounts of fine-grained material were treated to obtain a concentrate of the clay fraction (<2 μm) through wet sieving (<0.035 mm) followed by centrifugation according to Stokes' law.

The mineralogical composition was determined by X-ray diffraction (XRD). Diffractograms were obtained with an Aeris instrument (PanAlytical) equipped with a Cu tube, at 15 kV, 40 mA, 0.02173° step-size, and at a velocity of 3.3°/min. For both sand and mud deposits, bulk mineralogy was determined on ground (to <15 μm), randomly oriented grains in the range 2–60° 2θ. Clay mineralogy was determined on oriented aggregates, with measurements performed on air-dried slides (in the range 2–30° 2θ) and after solvation with ethylene-glycol and heating at 550°C (2–15° 2θ). After extracting the background, semi-quantitative estimates of mineral proportions were based on the areas of characteristic reflections identified in the diffractograms. Because of the uncertainties involved in semi-quantitative evaluations by XRD (Hillier, 2003; Moore & Reynolds, 1997), obtained results are estimates of mineral proportions.

Geochemistry was determined with the same aliquots used for bulk mineralogy (<0.035 mm for muds; <2 mm for sands). Analyses were performed after lithium metaborate/tetraborate fusion and nitric acid digestion at the laboratories of Bureau Veritas (Vancouver; group 4A-4B and code LF200). Major oxides and some minor-trace elements were determined by inductively coupled plasma-atomic emission spectroscopy (ICP-AES; using Spectro Ciros/Arcos equipment) and trace elements by ICP-mass spectrometry (ICP-MS; using an ICPMS ELAN 9000). Total iron was indicated in the form of Fe_2O_3. Most geochemical data were already presented in a previous article (Cruz et al., 2021).

Heavy minerals were retrieved from the fraction 0.063–0.5 mm of sand deposits, with the separation performed by the gravitational method using Na-polytungstate (*ca* 2.9 g/cm^3). The weight percentages of the 0.063–0.5 mm fraction and the heavy mineral concentrate in this fraction were recorded for all samples to estimate the proportion of heavy minerals in the sampled sands. Heavy mineral grains were then mounted on a glass slide with Canada Balsam and analysed using a petrographic microscope according to their optical properties. At least 100 translucent grains were point-counted for each slide to obtain approximate volume percentages, while opaque grains were counted separately.

3.3 | Data treatment

Quantification of the relative contributions of source units in the different parts of the basin was obtained using a provenance tracking technique. For this purpose, samples from sub-catchments (e.g. tributary samples) draining almost exclusively a single main geologic unit (i.e. felsic, mafic or sedimentary units) were used to establish end-member compositions. A selection of compositional features that can be used in provenance assessments, including geochemical (SiO_2, Al_2O_3, Fe_2O_3, MgO, CaO, Na_2O, K_2O, TiO_2, Th, U, Zr, Y, La, Sm, Eu, Gd, along with ratios Ti/U, Eu/U, Ti/Th, Zr/Ti, Zr/Th, Y/Eu, La/Sm, Gd/Lu), bulk XRD-mineralogy (quartz, K-feldspar, plagioclase) and heavy mineral (zircon, tourmaline, epidote, pyroxene) variables was considered.

The contributions of each end-member to the final point were estimated using the unmixing model developed in the R platform FingerPro (Lizaga et al., 2020). Prior to modelling contributions for deposits with relatively big catchment areas (12S, 20S, 37S), some statistical techniques were applied to maximise discrimination among the three sediment sources using the most adequate variables. These include: (1) the range test, which discards input parameters that have higher or lower content in the endpoint than in the sources; (2) the non-parametric Kruskal–Wallis *H* test to identify components that provide statistically significant discrimination (i.e. $p < 0.05$) between sources; (3) stepwise discriminant analysis based on Wilks' lambda minimisation (Collins et al., 2017).

4 | RESULTS

4.1 | Morphometry of the source areas

This section is focussed on the orographic features that may reflect regional differences in sediment production (Table 1; Figure 3). On average, the upstream reaches of the Caculuvar Basin are steeper than downstream regions with mafic and felsic basement rocks and, in particular, those placed in the Kalahari Basin. Except for some upstream sectors on the edge of mountain ranges, steeper slopes are usually found in the valley margins. Drainage density does not vary significantly from upstream to downstream locations of the drainage basin, being comparable in regions with distinct geological outcrops. However, it appears to be slightly higher in sectors with mafic rather than felsic basement rocks. On the other hand, relative relief and valley depth tend to be higher in sectors with felsic rather than mafic basement rocks. Highest values for these parameters are found at the transition between elevated regions of the Humpata–Bimbe plateau with metasedimentary units to the lower planation in granitoids and associated with inselbergs in areas with diverse crystalline rocks. As expected, relative relief and valley

TABLE 1 Summary data of geomorphic parameters and precipitation determined in areas with the main geological units of the Caculuvar–Mucope river system

	Slope (°)		Drainage density (km^{-1})		Relative relief (m)		Valley depth (m)		Rainfall (mm)	
	Max	$\overline{X}$	Max	$\overline{X}$	Max	$\overline{X}$	Max	$\overline{X}$	Max	$\overline{X}$
Sedimentary Meso-Cenozoic	46	1	2.5	1	161	50	64	18	923	712
Sedimentary metamorphic	55	5	1.63	0.83	547	223	114	27	994	871
Mafic crystalline	53	1	2.65	1.07	453	82	113	27	912	669
Felsic crystalline	54	3	1.94	0.91	563	142	120	32	979	849

depth are especially low in the overall flat region of the Kalahari Basin.

4.2 | Composition of fluvial sediments

4.2.1 | Dominated by felsic sources

The XRD-mineralogy of sands mainly sourced from felsic terrain reveals a clear prevalence of quartz (63%–90%) over feldspar (0%–27%) (Figure 4). The heavy mineral fraction usually yields high epidote content (33%–64%), occasionally with comparable amounts of zircon (7%–41%), and secondary amphibole (Figure 5). These results are in line with a previous investigation focussing on the petrography of river sands from south-west Angola (Garzanti et al., 2018a). Geochemically, sands derived from felsic sources are easily distinguished by their high K_2O (>2.8%) and Rb (>82 mg/kg) contents, and, in particular, the relatively low Ti compared to other high field strength elements with higher felsic affinity, namely Th and U (Figure 6). They are also distinguished by several features of the rare earth elements (REE) patterns, such as a negative Eu-anomaly ($0.51 < Eu/Eu^* < 0.79$), relatively high light REE fractionation ($5.02 < [La/Sm]_N < 5.92$) and flat heavy REE patterns ($0.88 < [Gd/Yb]_N < 1.60$) (Cruz et al., 2021).

Mud deposits tend to yield similar amounts of feldspar, with more K-feldspar than plagioclase, and quartz (Figure 4). They are depleted in SiO_2 and tend to be substantially enriched in Al_2O_3, REE, U and V relative to sands collected at the same site (Figure 6). The clay fraction of these deposits is usually dominated by kaolinite, followed by illite (Figure 7).

4.2.2 | Dominated by mafic sources

Mafic-derived sands tend to be dominated by feldspar, in general with a clear prevalence of plagioclase over K-feldspar, but streams draining small patches of felsic igneous rocks may contain comparable amounts of quartz and feldspar, with almost as much plagioclase as K-feldspar (Figure 4). A mafic-dominated source is clearly shown by the prevalence of pyroxene, mainly hypersthene (>75% of the translucent fraction), in heavy mineral suites, with secondary amounts of amphibole and epidote (Figure 5). Compared with sediments with felsic and sedimentary sources, mafic-derived sands yield low SiO_2 (<65%) and high contents of Al_2O_3 (>15%), CaO (>5%), Fe_2O_3 (>4%), TiO_2 (>1%) and MgO (>0.6%). The discrimination of these deposits is clearly accomplished with ratios of relatively non-mobile elements, namely using Eu, Sc, Th, Ti, Y and Zr (Figure 6).

The compositional information about fine-grained material is limited to the mineralogy of the clay fraction retrieved from sand deposits and mud deposits collected at the downstream limit of the Cunene Complex of south-west Angola. This mud contains similar amounts of plagioclase and quartz (Figure 4) and reveals relatively high contents of CaO (2.57%), MgO (1.35%) and Na_2O (0.89%). The clay fractions obtained from sand and mud samples yield minor or no illite and are usually dominated by smectite (up to *ca* 80%), but one sample collected in an upstream location is relatively rich in kaolinite (Figure 7).

4.2.3 | Dominated by sedimentary sources

Sedimentary-derived sands are characterised by high quartz contents (>90%) and almost no feldspars, while phyllosilicates occur in only minor amounts (Figure 4). The heavy mineral assemblages of sand samples collected in the Mucope sub-basin are dominated by zircon (50%–68%) followed by tourmaline (16%–24%). The effect of quartz dilution in recycled sediments is revealed by extremely high SiO_2 (>95%) and extremely low K_2O (<0.45%), and, in particular, Na_2O (<0.03%) and CaO (<0.05%). The abundance of minor elements that tend to be non-mobile is variable, but the Mucope sands tend to show enrichment in Zr

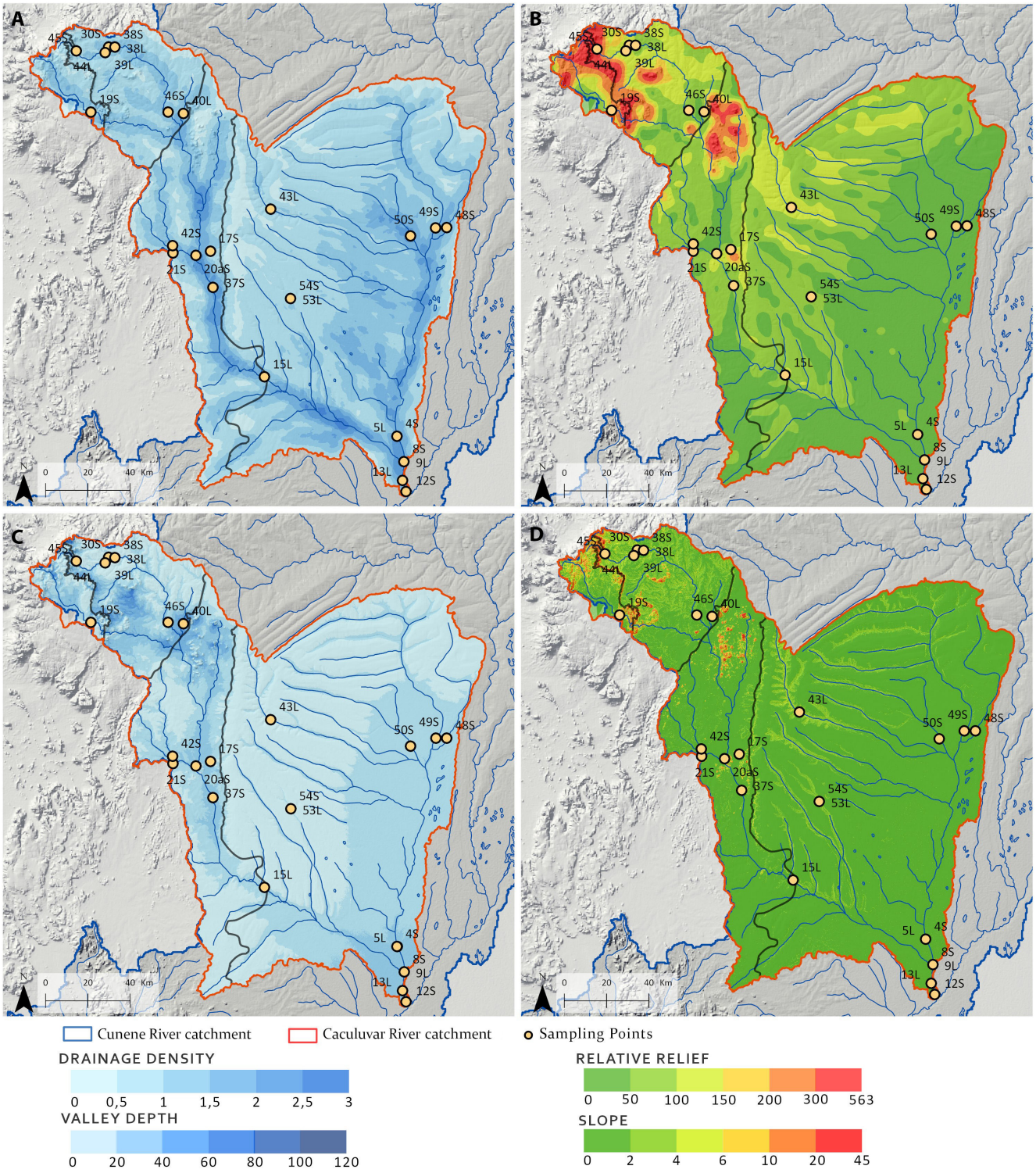

FIGURE 3 Geomorphic parameters that can be used as proxies of erosion for the Caculuvar–Mucope catchment areas. (A) Drainage density (km^{-1}), (B) valley depth (m), (C) relative relief (m) and (D) slope (°).

relative to other high field strength elements (e.g. Ti, Sc, REE) (Figure 6). The sample collected in the upper reaches of the Caculuvar River, where it is draining mainly sedimentary and metasedimentary successions with volcaniclastic intercalations of the Chela Group that are cut by hypabyssal doleritic rocks, has a distinct composition. It is distinguished by the presence of zircon and pyroxenes in similar amounts, yielding also slightly more Fe_2O_3, TiO_2 and REE than the other recycled sands.

Fine-grained deposits can be dominated by quartz (34%–73%) or phyllosilicates (24%–58%) and contain secondary to minor feldspar (Figure 4). As expected,

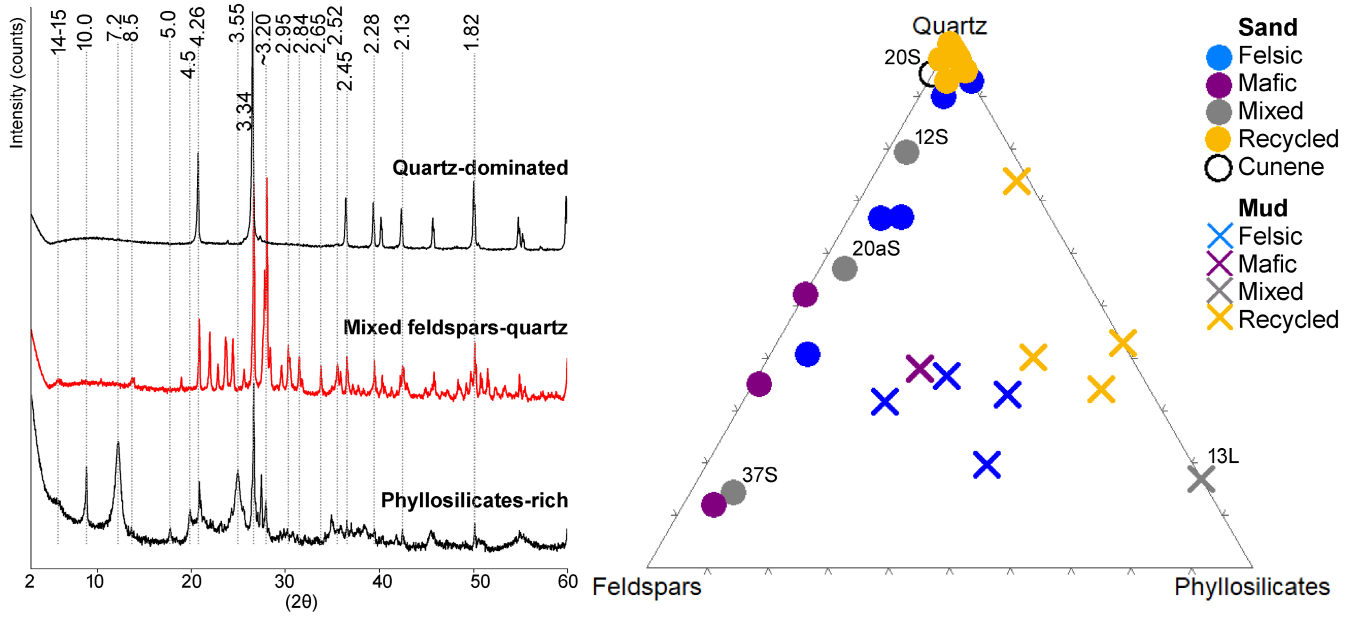

FIGURE 4 XRD bulk mineralogy obtained for sand and mud deposits. Samples with mixed source are identified. Note the strong quartz-domain in sands with an important recycled component, quartz to quartz-feldspar (mainly K-feldspar) if sources are predominantly felsic and high feldspar (mainly plagioclase) if sources are predominantly mafic. Muds contain substantially more quartz than feldspar only where the source area comprises sedimentary units.

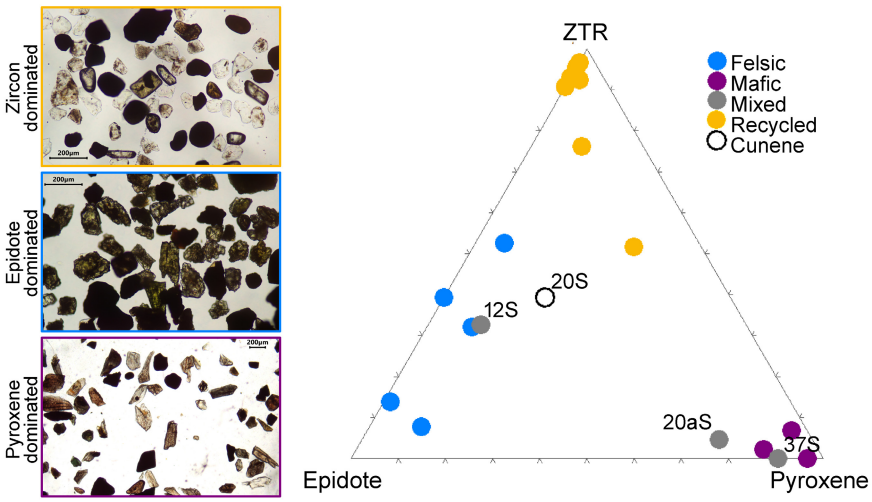

FIGURE 5 Heavy mineral assemblages of sand deposits. ZTR: zircon + tourmaline + rutile. Samples with mixed source are identified. Sediments mainly sourced by mafic units are strongly dominated by pyroxene. Sands mainly sourced by sedimentary units of the Kalahari Basin contain mainly zircon followed by tourmaline. Felsic-dominated sands yield high epidote or epidote and zircon in comparable amounts.

quartz-dominated sediments yield more silica, while alumina is more abundant in sediments rich in phyllosilicates, with all these sediments having in common low Na_2O contents (<0.25%). The clay fractions obtained from sand and mud deposits tend to be dominated by kaolinite (up to 92%), have minor illite and usually lack smectite (Figure 7).

4.2.4 | Mixed-sourced

Sands sourced by a combination of felsic, mafic and sedimentary units were sampled at four sites. One in Cunene, downstream of the Caculuvar confluence (20S), two in Caculuvar (upstream (37S) and downstream (12S) of the Mucope confluence), and one in a small tributary of Caculuvar (20aS). These samples are compositionally distinct, reflecting variable contributions from different source units.

The Cunene and lower Caculuvar sands are quartz-dominated (Figure 4), yielding very high silica (92%–93%), low Al_2O_3 (3%–4%), and less than 1% of all other chemical elements. Most ratios of non-mobile elements are comparable to those measured in sediments with a recycled source (Figure 6). In terms of heavy minerals, these sediments contain mainly epidote (50% in lower Caculuvar; 35% in Cunene) and zircon (27% in lower Caculuvar; 25% in Cunene), followed by pyroxenes and tourmaline

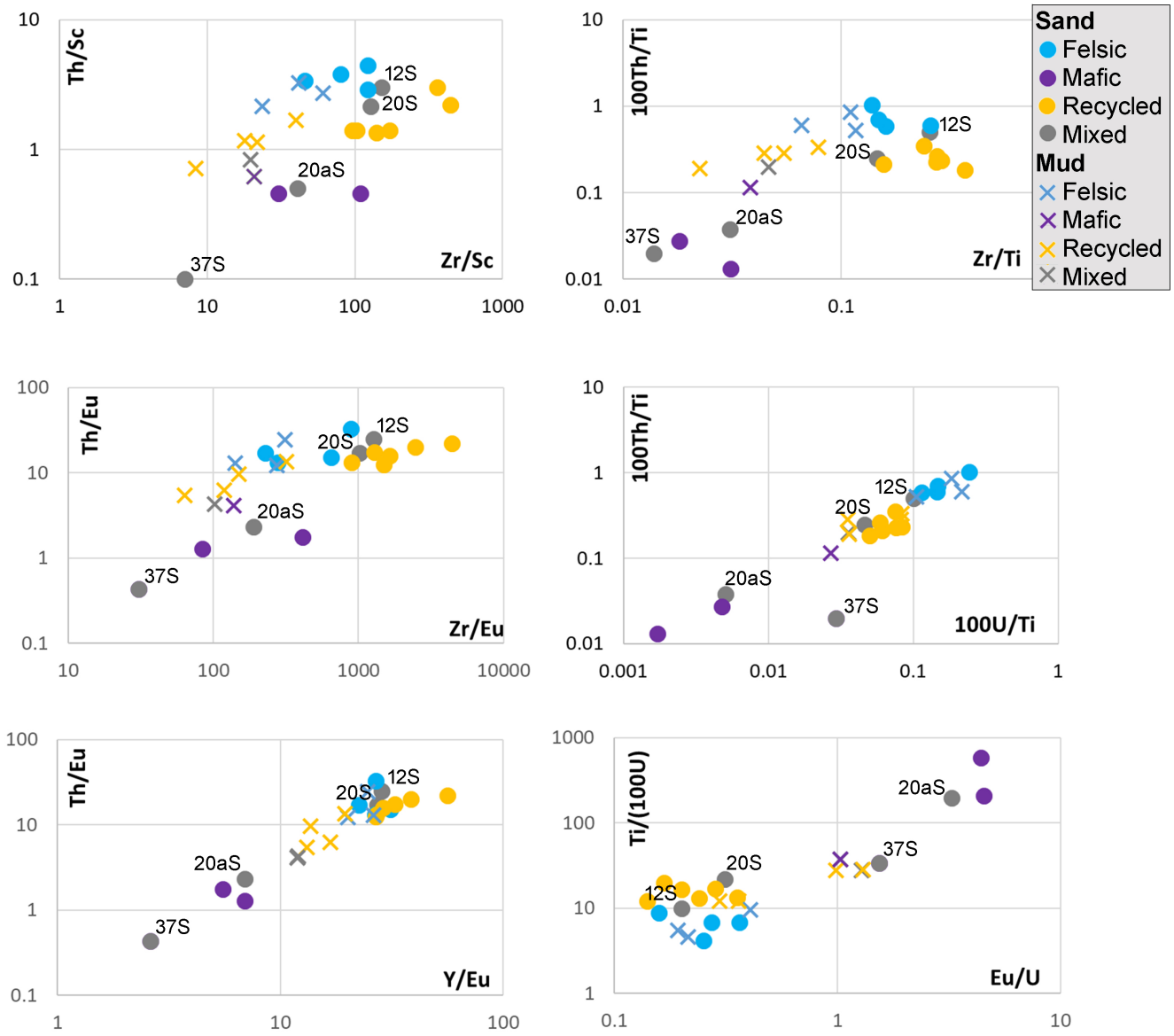

FIGURE 6 Scatter plots of non-mobile elements discriminating sediments according to their source area geology. Samples with mixed source are identified.

(Figure 5). Compared with these samples, the Caculuvar sand collected upstream of the Mucope confluence is depleted in SiO_2 (64.6%) and enriched in Al_2O_3 (20.3%), CaO (8.3%), and Na_2O (3.1%), displaying ratios of non-mobile elements (namely those that consider Ti, Zr, Th, Sc and REE) typical of deposits with a mafic source (Figure 6). Mineralogically, it contains much more feldspar (mainly plagioclase) than quartz (Figure 4), and the heavy mineral fraction comprises mostly pyroxene (85%), with epidote and amphiboles in secondary amounts (Figure 5). Sand collected in the tributary of Caculuvar has a composition between the previous two extremes (i.e. Cunene/lower Caculuvar and upper Caculuvar).

The clay fractions (separated from sand and mud deposits) of Cunene and lower Caculuvar sediments yield comparable amounts of kaolinite and smectite. Smectite tends to be dominant in river stretches placed in the Cunene Complex of south-west Angola, while in the upper reaches of Caculuvar kaolinite is dominant and illite can be the second most abundant mineral (Figure 7).

5 | DISCUSSION

5.1 | Signs of regionally variable sediment production

In the studied setting, felsic, mafic and recycled sources can be easily distinguished through sediment composition, making possible an assessment of the relative

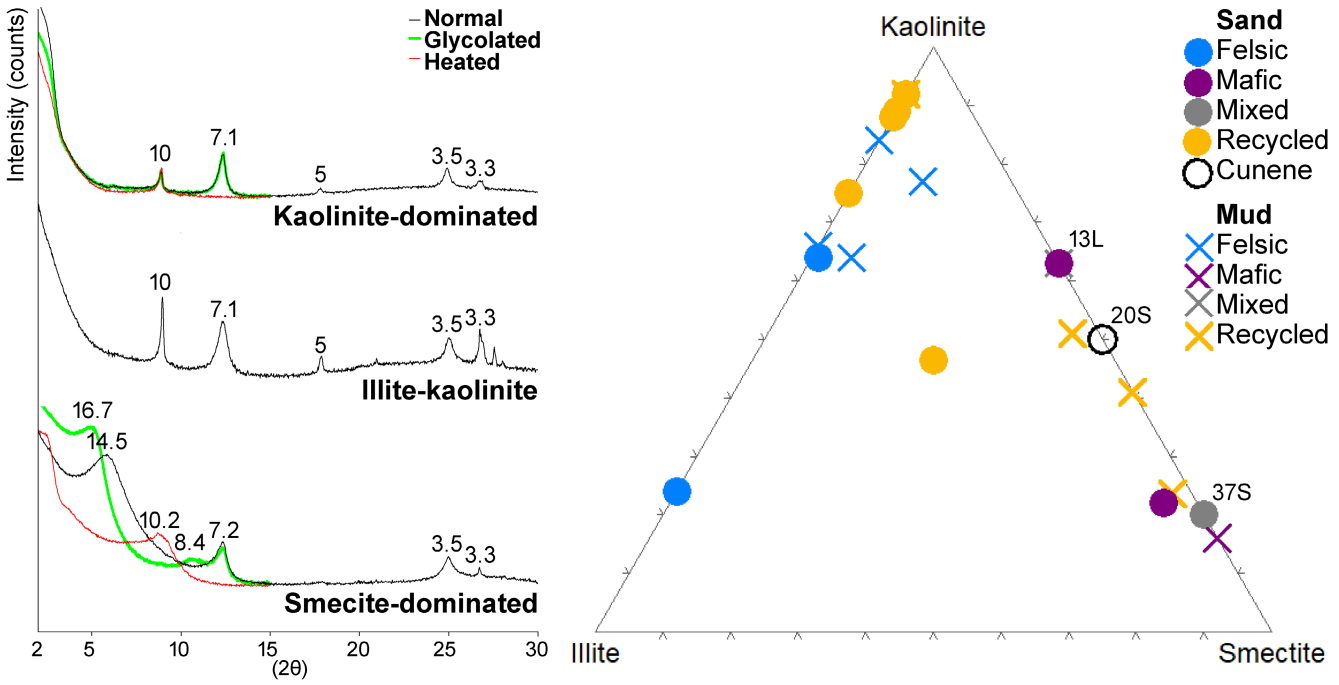

FIGURE 7 Clay mineralogy obtained for sand and mud deposits. Samples with mixed source are identified. Illite and smectite are more abundant where sources are dominantly felsic and mafic, respectively. Recycled deposits can be either dominated by kaolinite, smectite or comprise similar amounts of kaolinite, illite and smectite.

contribution from these main geological units in heterogeneous drainage basins. Comparison of provenance contributions based on different input parameters is always desirable to reduce uncertainties, which are usually higher whenever exogenous sedimentary processes affect end members differently. To minimise these effects, unmixing models based on heavy mineral suites, geochemistry and XRD-mineralogy were performed for the Caculuvar upstream of the Mucope confluence (37S), the most downstream sample of the Caculuvar–Mucope river system (12S) and the Cunene sand (20S).

Results obtained with heavy mineral data always indicate the highest mafic contributions of the three datasets, while XRD-mineralogy tends to indicate higher sedimentary contributions (Table 2). Due to the heavy mineral enrichment in deposits with a mafic source (1.45%–4.05%) relative to those sourced by felsic terranes (0.71%–1.65%) and, in particular, with significant contribution from the Kalahari Basin (0.06%–0.99%), it can be argued that heavy mineral assemblages, along with the geochemical features determined mostly by these minerals, are dampened by mafic contributions. On the other hand, as recycling contributes to quartz-enrichment (Garzanti et al., 2020; Suttner et al., 1981), this dataset can lead to some biased estimates toward sedimentary contributions.

It is worth noting that, for sand deposits with wide catchment areas in the Kalahari Basin (12S and 20S), the three compositional datasets indicate an under-supply from this unit and an over-supply from areas with felsic crystalline rocks (Table 2). Morphometric and climatic features of the drainage areas placed in different source units (Table 1) can be used to test if differences in source contributions can be ascribed to distinct geomorphologically-specific denudation. In the Kalahari Basin, rainfall is relatively low (712 mm compared with 849 mm falling on felsic units) and relief is flat (lower slope, relative relief and valley depth). As drainage density in the Kalahari Basin (1.00 km^{-1}) is slightly higher than in the felsic igneous basement (0.91 km^{-1}) and most deposits therein are not consolidated, diminished supply from the Kalahari Basin should be ascribed to its lower relief and drier conditions. Provenance budgets based on sediment composition that were performed for the Zambezi River, which also drains the Kalahari Basin, already suggested relatively minor production from this region (Garzanti et al., 2022). In Cunene (20S), where the Kalahari Basin reaches wetter areas, the modelled sedimentary contribution is substantially higher, reinforcing the evidence of major rainfall control over sediment yields.

The XRD-mineralogy (Figure 4), heavy mineral suites (Figure 5) and geochemistry (Figure 6) suggest an overwhelming mafic component in the Caculuvar sample upstream of the Mucope confluence despite the wider representation of felsic basement rocks in the catchment area (Figure 2). Because the composition of this sample is so typical of a mafic source, model contributions are difficult

TABLE 2 Percentage contributions from the main geological units estimated using geochemical analysis, heavy mineral composition and bulk XRD-mineralogy for sediments with mixed source. Goodness of fit (GOF) is the quality of the model performance

	GOF	Felsic	FelSD	Mafic	MafSD	Recycled	RecSD
12S Caculuvar (post-Mucope)							
Actual area		0.13		0.15		0.73	
Geochemistry	0.87	0.64	0.09	0.06	0.03	0.30	0.04
XRD-mineralogy	0.92	0.54	0.18	0.04	0.05	0.42	0.13
Heavy minerals	0.89	0.72	0.10	0.07	0.06	0.21	0.09
All datasets	0.85	0.67	0.08	0.05	0.03	0.28	0.07
20S Cunene							
Actual area		0.14		0.05		0.81	
Geochemistry	0.90	0.42	0.05	0.09	0.02	0.49	0.05
XRD-mineralogy	0.94	0.05	0.07	0.09	0.03	0.86	0.05
Heavy minerals	0.91	0.47	0.08	0.11	0.07	0.42	0.08
All datasets	0.89	0.38	0.07	0.08	0.03	0.54	0.06
37S Caculuvar (pre-Mucope)							
Actual area		0.42		0.40		0.18	
Geochemistry (1)	0.70	0.56	0.10	0.42	0.08	0.02	0.04
XRD-mineralogy	Not able to run, only K-feldspar remained						
Heavy minerals (2)	0.99	0.04	0.03	0.96	0.04	0.00	0.00
All datasets (3)	0.72	0.47	0.09	0.44	0.10	0.09	0.07

Note: (1) Only SiO_2, Fe_2O_3, CaO, TiO_2, Ti/U, Ti/Th, Zr/Th passed the statistical tests; (2) only tourmaline and epidote passed the statistical tests; (3) using geochemical and heavy mineral variables listed in (1) and (2).

SD refers to the standard deviation for each source component (felsic, mafic and recycled) obtained with the model.

to perform (few variables passed statistical tests and goodness of fit tends to be low; Table 2). Uneven sediment supply depending on the distance of the sampling site to different geological units may have been crucial here, as bedload deposits are representative of only a very limited portion of the drainage area (Hale & Plant, 1994; Ottesen et al., 1989), with proximal sources probably exerting a major influence on sediment composition.

5.2 | Selective depletion/enrichment through sedimentary processes

Between primary source materials and final daughter deposits, exogenous processes may alter sediment composition in multiple ways. With regard to physical processes, it is well known that sediment sorting, according to particle density, size and shape, plays a major influence on sediment composition (Bridge & Bennett, 1992; Garcia et al., 2004; Garzanti et al., 2018b; Slingerland, 1977). A selective loss of elements that tend to concentrate in fine-grained fractions is evident in several scatter plots of ratios of non-mobile elements (Figure 6). In particular, they clearly show that with sediment reworking a more pronounced decrease in Ti content occurs than in most other non-mobile elements. The mechanical disintegration of the most labile minerals may also change sediment composition. For example, a down-current decrease in feldspars relative to quartz was already attributed to mechanical breakdown (McBride et al., 1996; Savage et al., 1988), but previous works demonstrated that most minerals found in detrital frameworks resist ultralong transport (Garzanti et al., 2015).

Chemical weathering exerts a stronger influence on mud composition than on coarser deposits (Dinis et al., 2017, 2020; Guo et al., 2018). In warm and wet environments, it also affects sand material by promoting the destruction of unstable minerals with consequent enrichment in the most durable ones (Garzanti et al., 2013a; Johnsson et al., 1991; Le Pera et al., 2001). Weathering intensity associated with sediment production has been assessed with distinct geochemical and mineralogical features. Regarding mineralogy, the composition of the clay fraction was demonstrated to be the most reliable weathering proxy (Dinis et al., 2017; He et al., 2020). Clay assemblages also depend on source rock, but kaolinite tends to become more abundant regardless of parent material composition (Chamley, 1989; Velde, 1995). Numerous geochemical proxies of weathering intensity based on the relative proportions of a set of mobile and non-mobile elements have been proposed. Detailed descriptions of these parameters were provided elsewhere (Dinis et al., 2020;

Duzgoren-Aydin et al., 2002; Price & Velbel, 2003). In the present work, to accommodate the effect of the alteration of both feldspars and Fe/Mg primary minerals that are abundant in mafic rocks (e.g. olivines, pyroxenes, amphiboles), the Mafic Index of Alteration (MIA; Babechuk et al., 2014) was used. This parameter considers molar proportion and is obtained with the following formula designed for oxidising conditions:

$$\mathrm{MIA_o} = \left(\mathrm{Al_2O_3} + \mathrm{Fe_2O_3}\right) \times 100 / \left(\mathrm{Al_2O_3} + \mathrm{K_2O} + \mathrm{CaO^*} + \mathrm{Na_2O} + \mathrm{MgO}\right),$$

with CaO* being the silicate-bound carbonate.

Weathering extent can also be obtained for distinct mobile elements (e.g. K, Mg, Ca, Na, etc.), by measuring their levels of depletion through ratios of mobile element concentrations to those of Al_2O_3 normalised to the same ratio in a reference material ($\alpha^{Al}{}_E$; Garzanti et al., 2013b), such as the Upper Continental Crust (UCC; Rudnick & Gao, 2003). The formulation is:

$$\alpha^{Al}{}_E = (Al/E)_{sample} / (Al/E)_{UCC},$$

with E being a mobile element, with $\alpha^{Al}{}_E$ increasing with weathering intensity.

Recent works focussed on the composition of river muds from southern Africa have demonstrated climate to be a strong influence, despite the complexity raised by variable source geology (Dinis et al., 2017, 2020; Garzanti et al., 2014). In the studied area, reasonable correlations between different weathering proxies are observed for mud deposits (Figure 8). Dispersion increases significantly

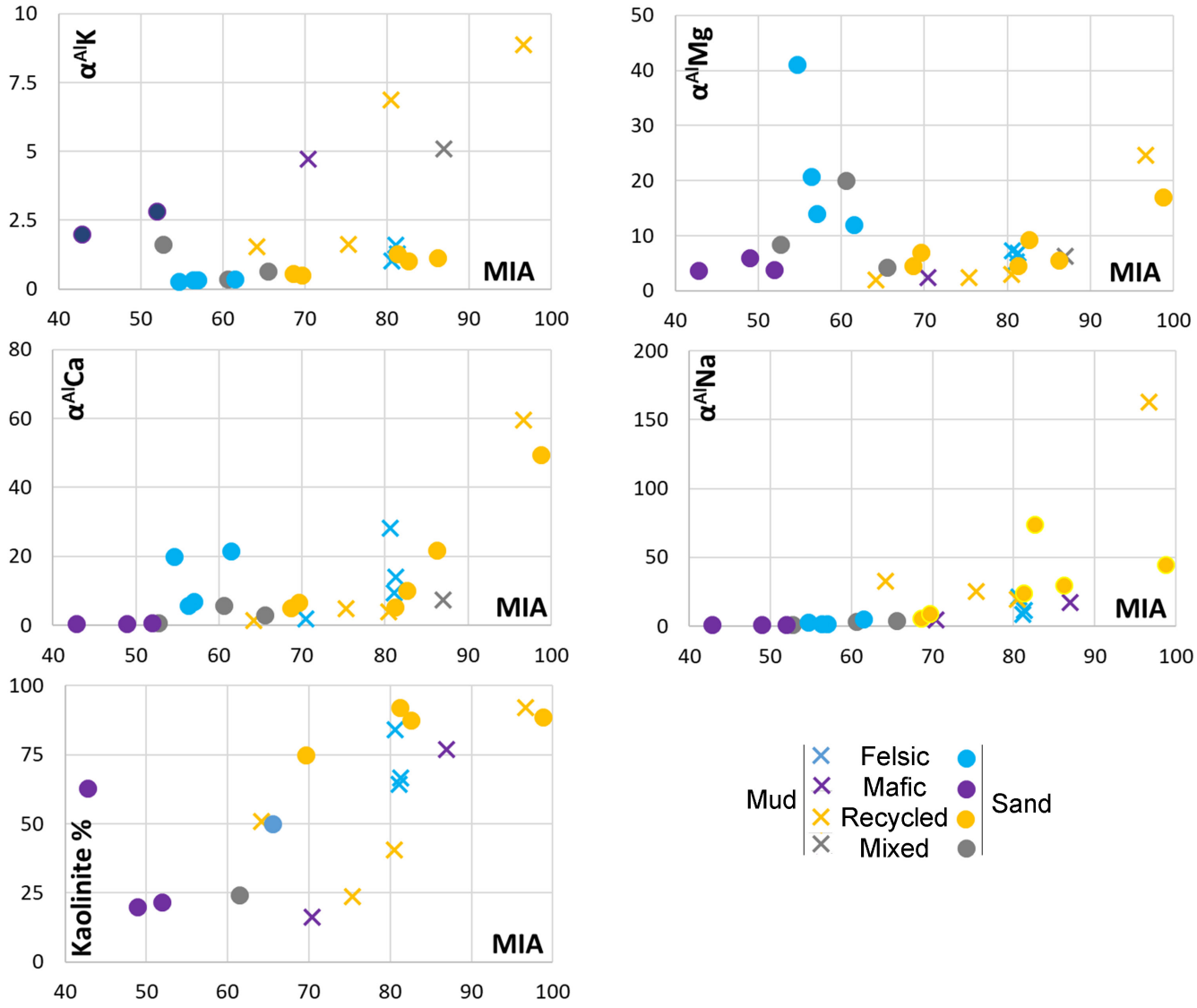

FIGURE 8 Weathering intensity determined from the geochemistry of mud deposits. Note the stronger link between MIA and most $\alpha^{Al}{}_E$ indices of element mobility for muds compared to sands and the highly variable values of the weathering proxies obtained with recycled muds.

in sands, with high $\alpha^{Al}{}_{K}$ where the source is mainly mafic and high $\alpha^{Al}{}_{Mg}$ and $\alpha^{Al}{}_{Ca}$ where the source is felsic. Such relationships demonstrate the strong compositional dependence of sand from source area geology. The heterogeneity in the values of the weathering proxies where the drainage basin spreads through sedimentary units reflects a complex recycling influence on sediment composition. Geochemically, the studied recycled muds are always strongly depleted in Na_2O, but not necessarily in CaO and MgO. Hence, recycling imposes major removal of Na, while other alkalis or alkaline-earth elements can be retained in secondary minerals formed during weathering. Namely, because Ca and Mg are frequently adsorbed on clay minerals (Chan et al., 1979; Cherian et al., 2018) and Mg is a common substitute in the octahedral sheet of smectites (Chamley, 1989; Velde, 1995).

The complexity introduced by recycling on weathering proxies is confirmed by the relationship between clay mineralogy and rainfall (Figure 9). Kaolinite contents in river deposits composed mainly of first-cycle detritus appear to correlate fairly well with rainfall in their respective catchment areas, but no relationship is seen for samples with a significant recycled component. In these deposits, part of the kaolinite must be inherited from the sedimentary source and not formed in the drainage areas during the last depositional cycle. A kaolinite enrichment in present-day deposits of the Zambezi River was already ascribed to inherence from sedimentary units notwithstanding regional wet and warm conditions prone to kaolinite formation (Garzanti et al., 2022).

Recycling also appears to be responsible for depletion in Ti and enrichment in Zr relative to source rocks; other elements that tend to be abundant in felsic rocks, such as U and Th, also tend to be lost through recycling (Figure 6). Variable depletion/enrichment can be ascribed to different physical and chemical exogenous processes. Chemically, pyroxene is among the most weathering

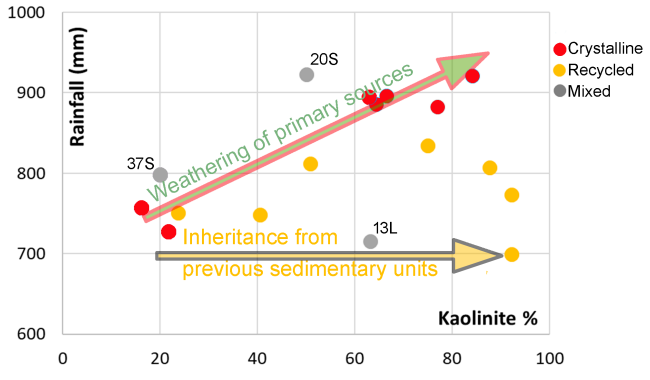

FIGURE 9 Relation between kaolinite percentages in the clay fraction of the sampled sediments and rainfall in their source areas. A possible relationship is lost where deposits include recycled material.

durable minerals of those derived from mafic-rocks (Eggleton et al., 1987; Nesbitt & Wilson, 1992), but it is not as stable under surface conditions as zircon, which is one of the most common transparent heavy minerals in the felsic-derived sands. In addition, some of the least mobile elements of the mafic component (e.g. Ti, Sc) tend to concentrate in fine-grained fractions that are easily entrained by the stream flow (Dinis et al., 2020), reducing their concentration in recycled deposits (Figure 6) and causing the mafic provenance signal to be more readily lost through recycling than the felsic signal.

6 | CONCLUSIONS

The Caculuvar River drainage basin, characterised by three source units yielding markedly distinct compositions (mafic, felsic and sedimentary), is ideal to estimate provenance budgets and evaluate exogenous transformations during a sediment cycle. Unmixing results obtained for sand deposits using different datasets diverge, with heavy mineral suites estimating higher mafic contributions and bulk XRD-mineralogy favouring sedimentary contributions. These differences are explained by the heavy mineral abundance in mafic rocks and the trend for quartz enrichment during depositional cycles. However, geochemistry, XRD-mineralogy and heavy mineral assemblages all point to a limited supply from the sedimentary units of the Kalahari Basin, despite their dominantly loose character and wide representation in Caculuvar and Cunene drainage basins. Conversely, the estimated contribution from mafic sources can be overwhelming in sites within outliers of these units, especially if assessed with heavy mineral assemblages. Such uneven detritus supply is ascribed to the pattern of rainfall distribution, varied relief in source areas and enhanced contribution from proximal sources. The obtained data also show that a possible association between sediment composition and (palaeo) environmental conditions is particularly difficult to perform where multiple depositional cycles are involved in sediment production. Namely, because composition may be partially inherited from previous-cycle deposits and exogenous processes affect differently detritus material sourced by mafic and felsic crystalline units.

This investigation with modern deposits revealed the extent to which variable sediment production and exogenous transformations during a sediment cycle can deviate the composition of the produced detritus from an average composition of source units weighted by their exposure areas. Hence, palaeogeographical interpretations based on the composition of sedimentary rocks can be significantly biased due to under/over-representation of some source components.

ACKNOWLEDGEMENTS

This investigation was supported by national funds through FCT—Foundation for Science and Technology, I.P., within the scope of the project UIDB/04292/2020 (MARE). P. Leite is thanked for her help in geomorphological characterisation. Early versions of the manuscript benefited from comments and suggestions by the Associate Editor Paul Carling and anonymous reviewers.

DATA AVAILABILITY STATEMENT

The data that support the findings of this study are available in the supplementary material of this article.

ORCID

Pedro Alexandre Dinis https://orcid.org/0000-0001-7558-7369

REFERENCES

Araújo, A.G., Guimarães, F., Perevalov, O.V., Voinovsky, A.S., Tselikovosky, A.F., Agueev, Y.L., Polskoi, F.R., Khodirev, V.L. & Kondrátiev, A.I. (1992) *Geologia de Angola – Notícia Explicativa da Carta Geológica de Angola à escala de 1:1000 000*. Luanda, Angola: Angolan Geological Services.

Arribas, J., Critelli, S. & Johnsson, M.J. (2007) *Sedimentary provenance and petrogenesis: perspectives from petrography and geochemistry*. Boulder, Colorado: Geological Society of America, p. 420.

Babechuk, M.G., Widdowson, M. & Kamber, B.S. (2014) Quantifying chemical weathering intensity and trace element release from two contrasting basalt profiles, Deccan Traps, India. *Chemical Geology*, *363*, 56–75.

Bridge, J.S. & Bennett, S.J. (1992) A model for the entrainment and transport of sediment grains of mixed sizes, shapes, and densities. *Water Resources Research*, *28*, 337–363.

Carvalho, H. (1984) Estratigrafia do Precâmbrico de Angola. *Garcia de Orta*, *7*(1–2), 1–66.

Carvalho, H., Tassinari, C., Alves, P., Guimarães, F. & Simões, M. (2000) Geochronological review of the Precambrian in Western Angola: links with Brazil. *Journal of African Earth Sciences*, *31*, 383–402.

Chamley, H. (1989) *Clay mineralogy*. Berlin: Springer.

Chan, K.Y., Davey, B.G. & Geering, H.R. (1979) Adsorption of magnesium and calcium by a soil with variable charge. *Soil Science Society of America Journal*, *43*, 301–304.

Cherian, C., Kollannur, N.J., Bandipally, S. & Arnepalli, D.N. (2018) Calcium adsorption on clays: effects of mineralogy, pore fluid chemistry and temperature. *Applied Clay Science*, *160*, 282–289.

Collins, A.L., Pulley, S., Foster, I.D.L., Gellis, A., Porto, P. & Horowitz, A.J. (2017) Sediment source fingerprinting as an aid to catchment management: a review of the current state of knowledge and a methodological decision-tree for end-users. *Journal of Environmental Management*, *194*, 86–108.

Cook, C., Reason, C. & Hewitson, B.C. (2004) Wet and dry spells within particularly wet and dry summers in the south African summer rainfall region. *Climate Research*, *26*, 17–31.

Correia, H. (1976) O Grupo da Chela e Formação da Leba como novas unidades litoestratigráficas resultantes da redefinição da Formação da Chela na região do Planalto da Humpata (Sudoeste de Angola). *Boletim da Sociedade Geológica de Portugal*, *20*, 65–130.

Cox, R., Lowe, D.R. & Cullers, R.L. (1995) The influence of sediment recycling and basement composition on evolution of mudrock chemistry in the southwestern United States. *Geochimica et Cosmochimica Acta*, *59*, 2919–2940.

Crétat, J., Pohl, B., Dieppois, B., Berthou, S. & Pergaud, J. (2019) The Angola low: relationship with southern African rainfall and ENSO. *Climate Dynamic*, *52*, 1783–1803.

Cruz, A., Dinis, P.A., Gomes, A. & Leite, P. (2021) Influence of sediment cycling on the rare-earth element geochemistry of fluvial deposits (Caculuvar–Mucope, Cunene River Basin, Angola). *Geosciences*, *11*, 384.

de Waele, B., Johnson, S.P. & Pisarevsky, S.A. (2008) Palaeoproterozoic to Neoproterozoic growth and evolution of the eastern Congo Craton: its role in the Rodinia puzzle. *Precambrian Research*, *160*, 127–141.

Dieppois, B., Rouault, M. & New, M. (2015) The impact of ENSO on Southern African rainfall in CMIP5 ocean atmosphere coupled climate models. *Climate Dynamic*, *45*, 2425–2442.

Dinis, P., Garzanti, E., Vermeesch, P. & Huvi, J. (2017) Climatic zonation and weathering control on sediment composition (Angola). *Chemical Geology*, *467*, 110–121.

Dinis, P.A., Garzanti, E., Hahn, A., Vermeesch, P. & Pinto, M.C. (2020) Weathering indices as climate proxies: A step forward based on Congo and SW African river muds. *Earth-Science Review*, *201*, 103039.

Dixon, J.L., Hartshorn, A.S., Heimsath, A.M., DiBiase, R.A. & Whipple, K.X. (2012) Chemical weathering response to tectonic forcing: a soils perspective from the San Gabriel Mountains, California. *Earth and Planetary Science Letters*, *323*, 40–49.

Drüppel, K., Littmann, S., Romer, R.L. & Okrusch, M. (2007) Petrology and isotopic geochemistry of the Mesoproterozoic anorthosite and related rocks of the Kunene intrusive complex, NW Namibia. *Precambrian Research*, *156*, 1–31.

Duzgoren-Aydin, N.S., Aydin, A. & Malpas, J. (2002) Re-assessment of chemical weathering indices: case study on pyroclastic rocks of Hong Kong. *Engineering Geology*, *63*, 99–119.

Eggleton, R.A., Foudoulis, C. & Varkevisser, D. (1987) Weathering of basalt: changes in rock chemistry and mineralogy. *Clays and Clay Minerals*, *35*, 161–169.

Ernst, R.E., Pereira, E., Hamilton, M.A., Pisarevsky, S.A., Rodriques, J., Tassinari, C.C., Teixeira, W. & Van-Dunem, V. (2013) Mesoproterozoic intraplate magmatic 'barcode' record of the Angola portion of the Congo Craton: newly dated magmatic events at 1505 and 1110 Ma and implications for Nuna (Columbia) supercontinent reconstructions. *Precambrian Research*, *230*, 103–118.

Feio, M. (1981) O relevo do sudoeste de Angola; estudo de geomorfologia. *Memórias da Junta de Investigações Científicas do Ultramar*, *67*, 1–67.

Florinsky, I.V. (2016) *Digital terrain analysis in soil science and geology*. Amsterdam, Netherlands: Elsevier. https://doi.org/10.1016/C2010-0-65718-X

Gabet, E.J. & Mudd, S.M. (2009) A theoretical model coupling chemical weathering rates with denudation rates. *Geology*, *37*, 151–154.

Gaillardet, J., Dupré, B. & Allègre, C.J. (1999) Geochemistry of large river suspended sediments: silicate weathering or

recycling tracer? *Geochimica et Cosmochimica Acta*, *63*, 4037–4051.

Garcia, D., Ravenne, C., Maréchal, B. & Moutte, J. (2004) Geochemical variability induced by entrainment sorting: quantified signals for provenance analysis. *Sedimentary Geology*, *171*, 113–128.

Garçon, M. & Chauvel, C. (2014) Where is basalt in river sediments, and why does it matter? *Earth Planetary Science Letters*, *407*, 61–69.

Garzanti, E., Padoan, M., Andò, S., Resentini, A., Vezzoli, G. & Lustrino, M. (2013a) Weathering and relative durability of detrital minerals in equatorial climate: sand petrology and geochemistry in the East African Rift. *The Journal of Geology*, *121*, 547–580.

Garzanti, E., Padoan, M., Setti, M., Peruta, L., Najman, Y. & Villa, I.M. (2013b) Weathering geochemistry and Sr-Nd isotope fingerprinting of equatorial upper Nile and Congo muds. *Geochemistry, Geophysics and Geosystems*, *14*, 292–316.

Garzanti, E., Padoan, M., Setti, M., López-Galindo, A. & Villa, I.M. (2014) Provenance versus weathering control on the composition of tropical river mud (southern Africa). *Chemical Geology*, *366*, 61–74.

Garzanti, E., Resentini, A., Andò, S., Vezzoli, G., Pereira, A. & Vermeesch, P. (2015) Physical controls on sand composition and relative durability of detrital minerals during ultra-long distance littoral and aeolian transport (Namibia and southern Angola). *Sedimentology*, *62*, 971–996.

Garzanti, E., Dinis, P., Vermeesch, P., Andò, S., Hahn, A., Huvi, J., Limonta, M., Padoan, M., Resentini, A., Rittner, M. & Vezzoli, G. (2018a) Dynamic uplift, recycling, and climate control on the petrology of passive-margin sand (Angola). *Sedimentary Geology*, *375*, 86–104.

Garzanti, E., Dinis, P., Vermeesch, P., Andò, S., Hahn, A., Huvi, J., Limonta, M., Padoan, M., Resentini, A., Rittner, M. & Vezzoli, G. (2018b) Sedimentary processes controlling ultralong cells of littoral transport: placer formation and termination of the Orange sand highway in southern Angola. *Sedimentology*, *65*, 431–460.

Garzanti, E., Vermeesch, P., Vezzoli, G., Andò, S., Botti, E., Limonta, M., Dinis, P., Hann, A., Baudet, D., de Grave, J. & Yaya, N.K. (2020) Congo River sand and the equatorial quartz factory. *Earth Science Reviews*, *197*, 102918.

Garzanti, E., Dinis, P., Vezzoli, G. & Borromeo, L. (2021) Sand and mud generation from continental flood basalts in contrasting landscapes and climatic conditions (Paraná–Etendeka conjugate igneous provinces, Uruguay and Namibia). *Sedimentology*, *68*, 3447–3475.

Garzanti, E., Bayon, G., Dinis, P., Vermeesch, P., Pastore, G., Resentini, A., Barbarano, M., Ncube, L. & Van Niekerk, H.J. (2022) The segmented Zambezi sedimentary system from source to sink: 2. Geochemistry, clay minerals, and detrital geochronology. *Journal of Geology*, *130*, 171–208.

Guo, Y., Yang, S., Su, N., Li, C., Yin, P. & Wang, Z. (2018) Revisiting the effects of hydrodynamic sorting and sedimentary recycling on chemical weathering indices. *Geochimica et Cosmochimica Acta*, *227*, 48–63.

Haddon, I.G. & McCarthy, T.S. (2005) The Mesozoic–Cenozoic interior sag basins of Central Africa: the Late-Cretaceous–Cenozoic Kalahari and Okavango basins. *Journal of African Earth Sciences*, *43*, 316–333.

Hale, M. & Plant, J.A. (1994) Drainage geochemistry. In: Govett, G.J.S. (Ed.) *Handbook of exploration geochemistry*. Amsterdam, Netherlands: Elsevier, p. 6.

Hanson, R. E., 2003. Proterozoic geochronology and tectonic evolution of southern Africa. In M. Yoshida, B. F. Windley, S. Dasgupta (Eds.) *Proterozoic East Gondwana: supercontinent assembly and breakup*, vol. *206*, London: Geological Society of London, pp. 427–463.

He, J., Garzanti, E., Dinis, P., Yang, S. & Wang, H. (2020) Provenance versus weathering control on sediment composition in tropical monsoonal climate (South China)-1 geochemistry and clay mineralogy. *Chemical Geology*, *558*, 119860.

Hillier, S. (2003) Quantitative analysis of clay and other minerals in sandstones by X-ray powder diffraction (XRPD). Clay mineral cements in sandstones. *International Association of Sedimentology Special Publication*, *34*, 213–251.

Huntley, B.J. (2019) Angola in outline: physiography, climate and patterns of biodiversity. In: Huntley, B., Russo, V., Lages, F. & Ferrand, N. (Eds.) *Biodiversity of Angola*. Cham: Springer, pp. 15–42.

Johnsson, M. J. & Basu, A. (Eds.) (1993) *Processes controlling the composition of clastic sediments*, vol. *284*. Boulder, Colorado: Geological Society of America.

Johnsson, M.J., Stallard, R.F. & Lundberg, N. (1991) Controls on the composition of fluvial sands from a tropical weathering environment: sands of the Orinoco River drainage basin, Venezuela and Colombia. *Geological Society of America Reports*, *103*, 1622–1647.

Le Pera, E., Arribas, J., Critelli, S. & Tortosa, A. (2001) The effects of source rocks and chemical weathering on the petrogenesis of siliciclastic sand from the Neto River (Calabria, Italy): implications for provenance studies. *Sedimentology*, *48*, 357–378.

Lizaga, I., Latorre, B., Gaspar, L. & Navas, A. (2020) FingerPro: an R package for tracking the provenance of sediment. *Water Resources Management*, *34*, 3879–3894.

Maharana, C., Srivastava, D. & Tripathi, J.K. (2018) Geochemistry of sediments of the peninsular rivers of the Ganga basin and its implication to weathering, sedimentary processes and provenance. *Chemical Geology*, *483*, 1–20.

Mayer, A., Hofmann, A.W., Sinigoi, S. & Morais, E. (2004) Mesoproterozoic Sm–Nd and U–Pb ages for the Kunene Anorthosite Complex of SW Angola. *Precambrian Research*, *133*, 187–206.

McBride, E.F., Abel-Wahab, A. & McGilvery, T.A. (1996) Loss of sand-size feldspar and rock fragments along the South Texas Barrier Island, USA. *Sedimentary Geology*, *107*, 37–44.

Moore, D.M. & Reynolds, R.C. (1997) *X-ray diffraction and the identification and analysis of clay minerals*. Oxford: Oxford University Press.

Morais, E., Sinigoi, S., Mayer, A., Mucana, A. & Rufino Neto, J. (1998) The Kunene gabbroanorthosite complex: preliminary results based on new field and chemical data. *African Geoscience Review*, *5*, 485–498.

Morton, A.C. & Hallsworth, C.R. (1999) Processes controlling the composition of heavy mineral assemblages in sandstones. *Sedimentary Geology*, *124*, 3–29.

Nesbitt, H.W. & Wilson, R.E. (1992) Recent chemical weathering of basalts. *American Journal of Science*, *292*, 740–777.

Ottesen, R.T., Bogen, J., Bölviken, B. & Volden, T. (1989) Overbank sediment: a representative sample medium for regional

geochemical mapping. *Journal of Geochemical Exploration*, *32*, 257–277.

Pereira, E., Tassinari, C.C., Rodrigues, J.F. & Van-Dúnem, M.V. (2011) New data on the deposition age of the volcano-sedimentary Chela Group and its Eburnean basement: implications to post-Eburnean crustal evolution of the SW of Angola. *Comunicações Geológicas*, *98*, 29–40.

Price, J.R. & Velbel, M.A. (2003) Chemical weathering indices applied to weathering profiles developed on heterogeneous felsic metamorphic parent rocks. *Chemical Geology*, *202*, 397–416.

Rasmussen, C., Brantley, S., Richter, D.D., Blum, A., Dixon, J. & White, A.F. (2011) Strong climate and tectonic control on plagioclase weathering in granitic terrain. *Earth and Planetary Science Letters*, *301*, 521–530.

Riebe, C.S., Kirchner, J.W. & Finkel, R.C. (2004) Erosional and climatic effects on longterm chemical weathering rates in granitic landscapes spanning diverse climate regimes. *Earth and Planetary Science Letters*, *224*, 547–562.

Rudnick, R.L. & Gao, S. (2003) Composition of the continental crust. In: Rudnick, R.L., Holland, H.D. & Turekian, K.K. (Eds.) *Treatise on geochemistry 3, the crust*. Pergamon, Oxford: Elsevier, pp. 1–64.

Savage, K.M. & Potter, P.E. (1991) Petrology of modern sands of the rios Guaviare and Inirida, southern Colombia: tropical climate and sand composition. *The Journal of Geology*, *99*, 289–298.

Savage, K.M., de Cesero, P. & Potter, P.E. (1988) Mineralogic maturity of modem sand along a high-energy tropical coast: Baixada de Jacarepegua, Rio de Janeiro, Brazil. *Journal of South American Earth Sciences*, *1*, 317–328.

Slingerland, R.L. (1977) The effects of entrainment on the hydraulic equivalence relationships of light and heavy minerals in sands. *Journal of Sedimentary Research*, *47*, 753–770.

Suttner, L.J., Basu, A. & Mack, G.H. (1981) Climate and the origin of quartz arenites. *Journal of Sedimentary Petrology*, *51*, 1235–1246.

Velde, B. (1995) *Origin and mineralogy of clays*. Berlin: Springer.

West, A.J., Galy, A. & Bickle, M. (2005) Tectonic and climatic controls on silicate weathering. *Earth and Planetary Science Letters*, *235*, 211–228.

SUPPORTING INFORMATION

Additional supporting information can be found online in the Supporting Information section at the end of this article.

How to cite this article: Cruz, A.T., Dinis, P.A., Lucic, M. & Gomes, A. (2023) Spatial variations in sediment production and surface transformations in subtropical fluvial basins (Caculuvar River, south-west Angola): Implications for the composition of sedimentary deposits. *The Depositional Record*, *9*, 83–98. https://doi.org/10.1002/dep2.208